Secular motion of three-dimensional Rydberg states in a microwave field

Andreas Buchleitner[1] and Dominique Delande[2]
[1]*Max-Planck-Institut für Quantenoptik, Hans-Kopfermann-Strasse 1, D-85478 Garching, Germany*
[2]*Laboratoire Kastler Brossel, 4, place Jussieu, Tour 12, 1^er Étage, F-75252 Paris Cedex 05, France*
(Received 12 April 1996)

We study the spectral properties of three-dimensional Rydberg states of atomic hydrogen in a microwave field of linear polarization. We identify a novel structure in the Floquet spectrum as the ''backbone'' of the experimentally observed ionization process. Localization properties, energies, *and lifetimes* of the individual Floquet states are shown to faithfully reflect the structure of classical phase space, which can be described by a perturbative approach. [S1050-2947(97)50902-4]

PACS number(s): PACS: 32.80.Rm, 05.45.+b, 42.50.Hz

The ionization of atomic Rydberg states by microwave fields allows for the experimental and theoretical study of quantum transport under the condition of highly nonlinear interaction between the atomic degrees of freedom and the driving field. In a classical picture, the ionization of the Rydberg electron is due to chaotic transport in classical phase space [1], within a wide range of microwave frequencies. As chaos is created for classical initial conditions *along* the z axis (parallel to the microwave field axis), it has been argued that chaotic ionization will merely reflect the dynamics along this one-dimensional subspace of three-dimensional (3D) configuration space [1,2]. In a quantum description, classical chaos manifests itself in a strong mixing of the unperturbed atomic eigenstates and the partial loss of good quantum numbers [1,3]. Extreme parabolic states (elongated along the polarization axis) are most strongly affected by the chaotic excitation in energy, since they most effectively populate initial conditions that correspond to classically chaotic motion [1,2,4]. In a more traditional language, they exhibit the largest oscillating dipole and therefore most effectively interact with the driving field. Consequently, experimental ionization thresholds [5,6] observed for a mixture of angular momentum or parabolic states distributed over the energy shell labeled by the principal quantum number n display globally quasi-one-dimensional behavior, since exactly the extreme parabolic states ionize first [2]. In view of the available experimental data, most of the theoretical emphasis [1,2,4] has so far been devoted to the atomic excitation in energy (i.e., in n), which, on the experimental time scales, could be shown [1,4] to be largely unaffected by the excitation in the transverse degree of freedom (angular momentum l).

It is the purpose of the present Rapid Communication to reveal the ''backbone'' of the quantum-mechanical ionization process by focusing exactly on this transverse dimension of phase space, which will allow us to identify a novel structure in the *exact quantum spectrum*. Whereas up to now the extreme parabolic state has been understood to be the *most fragile* under external driving [1], we shall describe *eigenstates of the unperturbed hydrogen atom* that are essentially *unaffected* by the microwave field, due to their symmetry properties, which are compatible with the dynamical symmetry of the Coulomb problem *as well as* with the symmetry imposed on the atom by the external perturbation. Note that the dynamical symmetry is a particular property of the hydrogen atom [7] and therefore *a priori not* applicable to nonhydrogenic Rydberg states, e.g., that of rubidium [8]. For the sake of a simple and transparent classical motivation of our quantum results we focus on microwave frequencies that are *nonresonant* with the unperturbed Kepler motion of the Rydberg electron.

The Hamiltonian describing the hydrogen atom in a monochromatic, linearly polarized microwave field of constant amplitude F and frequency ω reads, in the length gauge and in atomic units,

$$H=\frac{\mathbf{p}^2}{2}-\frac{1}{r}+Fz\,\cos\omega t. \tag{1}$$

As described in earlier work, a complex dilation of the corresponding Floquet Hamiltonian allows us to obtain the energies, the ionization rates, and the associated Floquet eigenstates of the atom dressed by the microwave photons [3]. Due to the azimuthal symmetry around the z axis, the problem is effectively 2D with a 5D phase space (because of the explicit time dependence of H). For vanishing microwave amplitude, the dressed eigenstates are products of spherical (n,l,m) states with Fock states of photon number K, where we choose $m=0$ for the conserved magnetic quantum number. For nonresonant microwave frequency, each energy level (n,K) has a degeneracy equal to the principal quantum number n in the angular momentum $0\leqslant l\leqslant n-1$. For nonvanishing field amplitude, the term $Fz\,\cos\omega t$ in the Hamiltonian couples different states with the selection rules $\Delta l=\pm 1$, $\Delta K=\pm 1$. To first order in F, there is no coupling inside the (n,K) manifold and the degeneracy is not lifted. To second order, there are nonzero terms that couple the state (n,l,K) to the states $(n,l\pm 2,K)$, through the intermediate states $(n',l\pm 1,K\pm 1)$; these terms lift the degeneracy. A crucial point is that the second-order term is *not diagonal* in l. The actual eigenstates of the 3D atoms dressed by the microwave field are consequently not (n,l,K) states, even *at lowest nonvanishing order*.

From a classical point of view, the electronic trajectories are simple Kepler ellipses, for $F=0$. For nonvanishing field amplitude, the nonresonant situation studied here corresponds to an electron on its Kepler orbit exposed to a microwave field oscillating at a noncommensurate frequency.

Hence, the electron cannot efficiently exchange energy with the field. To first order, it exhibits oscillations (driven by the microwave field) around its unperturbed Kepler ellipse. To second order, the resulting trajectory is an instantaneous elliptical trajectory, the parameters (eccentricity, spatial orientation) of which slowly evolve in time. This secular motion [9] preserves energy (the classical analog of n remaining an approximate good quantum number) and can be described by an effective Hamiltonian, after appropriate averaging over the oscillation of the microwave field [10]. The expansion of (1) in the canonical action-angle coordinates n (total action), θ (conjugate angle), l (angular momentum), and ψ (conjugate angle measuring the angle between the z axis and the major axis of the ellipse) of the hydrogen atom [1] reads

$$H=-\frac{1}{2n^2}+Fn^2\cos\omega t \times\sum_{M\geqslant 0}\{a_M(L_0)\cos M\theta\cos\psi+b_M(L_0)\sin M\theta\sin\psi\}. \quad (2)$$

$L_0=l/n$ is the scaled angular momentum,

$$a_M(x)=-\frac{2J'_M(M\sqrt{1-x^2})}{M}\quad (M\neq 0),\quad a_0=\tfrac{3}{2}\sqrt{1-x^2},$$

$$b_M(x)=\frac{2xJ_M(M\sqrt{1-x^2})}{M\sqrt{1-x^2}}\quad (M\neq 0),\quad b_0=0, \quad (3)$$

J_M represents the Bessel function, and the prime denotes the derivative. At lowest nonvanishing order in F we obtain

$$\overline{H_2}=\frac{F^2n^6}{8}\{h_1(L_0,\omega_0)\cos^2\psi+h_2(L_0,\omega_0)\sin^2\psi\}, \quad (4)$$

where $\omega_0=\omega n^3$ is the scaled frequency (ratio of the microwave to the Kepler frequency), and

$$h_1=\sum_{M\geqslant 0}\left(\frac{M^2(a_M^2-2L_0a_Ma'_M)-2Ma_Mb'_M}{\omega_0^2-M^2}-\frac{6M^4a_M^2}{(\omega_0^2-M^2)^2}\right). \quad (5)$$

Here, a_M and b_M are evaluated for the argument $L_0=l/n$. h_2 is obtained by exchanging a_M and b_M in (5). The lower-order terms of the effective Hamiltonian in F read $\overline{H_0}=-1/2n^2$ and $\overline{H_1}=0$.

The secular electronic motion as the temporal evolution of the conjugate variables l and ψ, generated by $\overline{H_2}$, can be represented by the motion of the vector (L_0,A_ρ,A_z) on the unit sphere. A_z and A_ρ design the components of the Runge-Lenz vector (directed along the major axis of the ellipse with a modulus equal to its eccentricity), defined by

$$A_z^2=(1-L_0^2)\cos^2\psi;\quad A_\rho^2=(1-L_0^2)\sin^2\psi. \quad (6)$$

In Fig. 1 we show several isovalue curves of $\overline{H_2}$ plotted on the unit sphere, for $\omega_0=1.304$. The figure is independent of the field strength and, thanks to classical scaling, independent of n, but it *changes* with ω_0. The value of ω_0 chosen here was motivated by experiments performed by the Stony Brook group [5]. One immediately recognizes that the motion is equivalent to that of a rigid rotor or a top, with three fixed points, that is three distinct types of classical periodic motion. The first two defined by $L_0=1$ and $A_\rho=1$ are stable. They correspond to the circular orbit in the plane containing the field polarization vector and to the straight-line orbit normal to that plane. The third fixed point defined by $A_z=1$ corresponds to the straight-line orbit along the field direction—the precise analog to the restricted 1D dynamics of the atom—and is *unstable*: an initial trajectory close to the field axis will diverge from it.

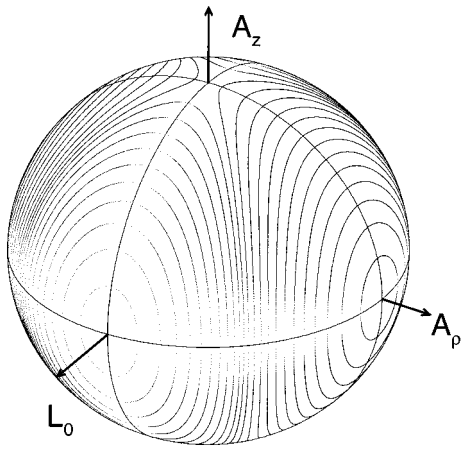

FIG. 1. Isocurve values for the effective Hamiltonian $\overline{H_2}$ describing the secular motion of a classical elliptical trajectory—represented (on the unit sphere) by its angular momentum L_0, and the parallel and perpendicular components A_z and A_ρ of the Runge-Lenz vector—under the influence of a linearly polarized microwave field of scaled frequency $\omega_0=1.304$. There are two stable ($A_\rho=1$ and $L_0=1$) fixed points corresponding to electronic motion along a straight line in the plane defined by the polarization vector of the microwave field and along a circle in a plane that contains the polarization vector, respectively. The third fixed point ($A_z=1$) is unstable and represents electronic motion along the polarization axis.

We can now predict the quantum spectrum of the atom dressed by the microwave field, by WKB quantization of $\overline{H_2}$. The semiclassical energies are defined by

$$\oint l\,d\psi=p+\tfrac{1}{2}, \quad (7)$$

the integral being evaluated along a classical secular trajectory (fixed value of $\overline{H_2}$) and p an integer ranging from 0 to $n-1$. This gives the 23 isovalue curves shown in Fig. 1 for the $n=23$ Rydberg manifold. The validity of this approach can be tested by a direct comparison to the ''exact'' numerical quantum spectrum. Indeed, after diagonalization of (1), one finds ''multiplets'' that originate from the unperturbed energy levels. The energies of these states are plotted in Fig. 2(a) for $n=23$, $F_0=Fn^4=0.03$, $\omega_0=1.304$, and compared to the semiclassical prediction. The agreement is quite good, with some quantitative disagreement for the lower part of the manifold. For both, the semiclassical and the exact result, there are ten eigenstates (labeled $p=0$ to 9 by increasing energy) corresponding to secular motion around the $L_0=1$ fixed point, and 13 eigenstates (from $p=10$ to 22) corre-

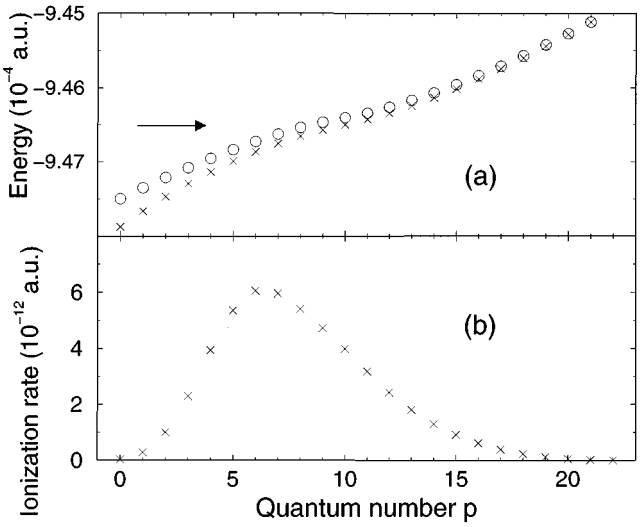

FIG. 2. Energy levels (originating from the $n=23$ manifold) of a hydrogen atom exposed to a microwave field with scaled frequency $\omega_0=1.304$ and scaled field $F_0=0.03$. (a) Comparison between the exact energy levels obtained from numerical diagonalization (crosses) and the semiclassical prediction using the effective Hamiltonian $\overline{H_2}$ (circles); the lowest (highest) energy levels $p=0$ to 9 (10 to 22) correspond to states localized around the fixed point $L_0=1$ ($A_\rho=1$) in Fig. 1; the arrow indicates the position of the corresponding energy level for the 1D model of the atom. (b) Ionization rates obtained from numerical diagonalization. There is a sharp maximum for states localized in the vicinity of the microwave field axis.

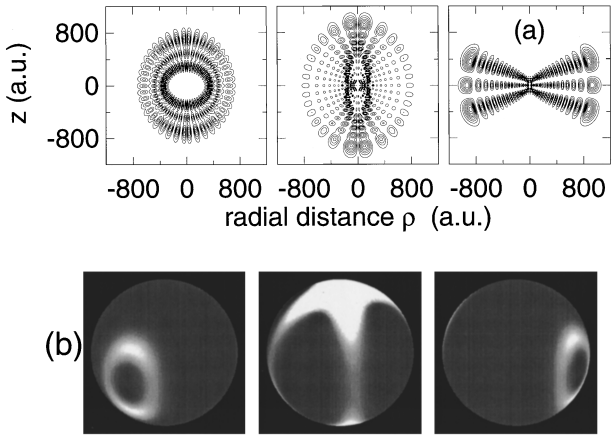

FIG. 3. (a) Isovalue curves for the electronic densities (averaged over one field period) of three eigenstates $p=2$, 8, and 20 (from left to right) of Fig. 2; as predicted by the secular calculation (see text), they are localized near a circular orbit, the field axis, and the plane perpendicular to the field, respectively; only the $p=8$ state significantly contributes to the ionization yield. (b) Husimi phase-space densities for the same three states plotted with the same coordinates as in the classical picture, Fig. 1 (density increases from black to white); the densities are well localized in the vicinity of the classical isocurves of $\overline{H_2}$, which proves that the second-order secular approximation describes the exact eigenstates quite well.

sponding to motion around the $A_\rho=1$ fixed point. The two series are separated by a minimum in the energy spacing, the quantum consequence of the slowing down of the classical motion [1,4] near the unstable fixed point. As indicated by an arrow in Fig. 2(a), it is *exactly* at this energy, which separates the L_0 and the A_ρ motion, that we find the Floquet eigenstate originating from $n=23$, in the restricted 1D dynamics. The semiclassical structure of the manifold is also reflected by the ionization rate of the individual Floquet states, as shown in Fig. 2(b) [11]. The states with pronounced L_0 or A_ρ character have extremely small ionization rates, the A_ρ states being actually more stable than the L_0 states. On the other hand, the states that correspond to motion close to the unstable fixed point exhibit the largest ionization rates. Yet, the maximum ionization rate is not observed for the eigenstate that comes closest to A_z motion, i.e., to the restricted 1D dynamics, but slightly is displaced to p values *below* the separatrix. According to our present accumulated numerical data (for different values of F_0, ω_0, and n), this displacement towards L_0 motion seems systematic but is not yet understood. However, for a broad distribution of atomic initial states over the n manifold [5,6], this does not affect the quasi-one-dimensional behavior of the ionization thresholds. Note, however, that at $F_0=0.03$ the ionization rate of the corresponding eigenstate of the 1D model is found to be two orders of magnitude smaller than the maximum ionization rate observed in Fig. 2(b). 1D and 3D widths acquire comparable values only in the vicinity of the 10% ionization threshold, i.e., at $F_0\simeq 0.05$ [3,5], when strong n mixing prevails. This and the displacement of the maximum width of the 3D manifold with respect to the separatrix may be an indication of the existence of an additional ionization channel due to the higher dimensionality of the real problem with respect to the restricted dynamics, in the case of near-integrable classical motion [10]. It provides a non-negligible correction to the popular 1D picture of the ionization process [1,4].

A further test of our semiclassical picture is to investigate the localization properties of the quantum eigenstates in configuration and in phase space. This is done in Fig. 3 for the states with $p=2,8,20$. The plots are contours of the electronic densities averaged over one field period, and of their phase-space Husimi densities on the surface of the unit sphere of Fig. 1. As expected, the state $|p=2\rangle$ is localized close to the circular orbit, $|p=8\rangle$ near the field axis, and $|p=20\rangle$ close to the plane perpendicular to the field. The associated phase-space densities are well localized in the vicinity of the isovalues of $\overline{H_2}$; that is, in the vicinity of the classical invariant tori, as expected from the semiclassical analysis. Let us mention that the states $|p=2\rangle$ and $|p=20\rangle$ are almost pure eigenstates of the unperturbed hydrogen atom [7]. Whereas $|p=2\rangle$ is very similar to $|n,l=n-2,m=0\rangle$, $|p=20\rangle$ can be obtained from the simultaneous diagonalization of the unperturbed Hamiltonian H_0, L_z, and $A_\rho^2+L_z^2\equiv\vec{\lambda}^2$. In this basis, $|p=20\rangle$ is practically identical to $|n,\lambda=n-3,m=0\rangle$. However, as the field amplitude is increased, the quiver amplitude of the electron [12] will tend to values that are comparable to the diameter of the state $|n,l=n-2,m=0\rangle$, leading to a hard transition from regular to chaotic motion for such high-angular-momentum states with $m=0$ (for classical studies, see [13]) and hence to the ionization of states like $|p=2\rangle$. A similar geometrical limitation does not exist for ''flat'' states like $|p=20\rangle$ that

do probe the Coulomb singularity, but are compatible with the cylindrical symmetry imposed by the driving field. This might explain the fact that flat electronic densities are systematically more stable against ionization than states like $|p=2\rangle$. In an ''exact'' numerical calculation we checked that the distribution of the widths of Fig. 2 and the associated classification of initial atomic states according to their symmetry properties correctly predict the relative ionization threshold of an extreme parabolic state, a high-angular momentum state $|n_0,l_0=n_0-1,m_0=0\rangle$, and a flat state $|n_0,\lambda_0=n_0-1,m_0=0\rangle$, which increases in the given order.

In conclusion, the quasi-one-dimensional ionization of 3D Rydberg states of atomic hydrogen is embedded in a transverse structure of 5D phase space, which can be described perturbatively. In future experiments, the details of this structure can be revealed by careful preparation of the atoms in well-defined initial states, such as $|n_0,l_0=n_0-1,m_0=0\rangle$ or $|n_0,\lambda_0=n_0-1,m_0=0\rangle$. Since these two states evolve into the states $|p=0\rangle$ and $|p=n_0-1\rangle$ in Fig. 2, we expect them to exhibit a dramatically smaller ionization yield than in current experiments that populate a mixture of Floquet states with an effective ionization yield dominated by intermediate p values.

A complementary experimental approach consists in direct photospectroscopy of the Floquet spectrum from low-lying atomic states. In this kind of experiment, the underlying phase-space geometry should be manifest in the positions and widths of the atomic resonances.

When Rydberg states of a different atomic species are used [8], the interaction of the electron with the ionic core should destroy the multiplets and produce Floquet eigenstates with completely different localization properties, since the described organization of the resonances strongly relies on the degeneracy of the energy levels of the hydrogen atom. This may explain why the experimentally observed ionization yields considerably differ from the ones obtained from hydrogen.

We acknowledge fruitful discussions with Jakub Zakrzewski and Howard Taylor. CPU time has been provided by IDRIS and RZG. Laboratoire Kastler-Brossel, de l'École Normale Supérieure et de l'Université Pierre et Marie Curie, is unité associée 18 du CNRS.

[1] G. Casati, B. V. Chirikov, I. Guarneri, and D. L. Shepelyansky, Phys. Rev. Lett. **59,** 2927 (1987); G. Casati, I. Guarneri, and D. L. Shepelyansky, IEEE J. Quant. Electron. **24,** 1420 (1988).

[2] R. Blümel and U. Smilansky, Z. Phys. D **6,** 83 (1987); R. V. Jensen, S. M. Susskind, and M. M. Sanders, Phys. Rev. Lett. **62,** 1476 (1989).

[3] A. Buchleitner, D. Delande, and J.–C. Gay, J. Opt. Soc. Am. B **12,** 505 (1995).

[4] J. G. Leopold and D. Richards, J. Phys. B **20,** 2369 (1987).

[5] P. M. Koch and K. A. H. van Leeuwen, Phys. Rep. **255,** 289 (1995), and references therein.

[6] J. E. Bayfield, CHAOS **1,** 110 (1991).

[7] D. Delande and J. C. Gay, J. Phys. B **17,** 335 (1984).

[8] M. Arndt, A. Buchleitner, R. N. Mantegna, and H. Walther, Phys. Rev. Lett. **67,** 2435 (1991).

[9] B. I. Meerson, E. A. Oks, and P. V. Sasorov, J. Phys. B **15,** 3599 (1982).

[10] A. J. Lichtenberg and M. A. Lieberman, *Regular and Stochastic Motion*, (Springer-Verlag, New York, 1983).

[11] Y. Bai, G. Hose, C. W. McCurdy, and H. S. Taylor, Chem. Phys. Lett. **99,** 342 (1983).

[12] R. Shakeshaft, Comm. J. Phys. B **28,** 179 (1992).

[13] F. Benvenuto, G. Casati, and D. L. Shepelyansky, Phys. Rev. A **45,** R7670 (1992).